Pure Appl. Chem., Vol. 84, No. 4, pp. 965–978, 2012.
http://dx.doi.org/10.1351/PAC-CON-11-08-20

Linear aromatic amide foldamer-derived supramolecular architectures and materials*

Zhan-Ting Li[1,2,‡], Kang-Da Zhang[2], Zhu-Ming Shi[2], Lu Wang[2], Cen Zhou[2], and Ben-Ye Lu[2]

[1]Department of Chemistry, Fudan University, Shanghai 200433, China; [2]State Key Laboratory of Bioorganic and Natural Products Chemistry, Shanghai Institute of Organic Chemistry, Chinese Academy of Sciences, 345 Lingling Lu, Shanghai 200032, China

Abstract: Intramolecular hydrogen bonding in oligomeric aromatic amides may induce the backbones to adopt folded, zigzag, or other extended conformations, depending on the positions of the amide units and the hydrogen-bonding sites on the aromatic rings. This article summarizes our efforts in exploring the applications of this family of preorganized oligomers in supramolecular and materials chemistry. Several series of preorganized frameworks or foldamers have been developed as efficient acyclic receptors for binding both neutral and ionic guests. The backbones have been modified with discrete functional groups from the ends or the side chains. The resulting molecules have been applied for designing new molecular tweezers, assembling ordered supramolecular architectures (organogels and vesicles), and directing the formation of complicated macrocyclic and capsular systems. When the hydrogen-bonded folded segments are connected to *n*-butyl methacrylate copolymers as cross-links, the resulting copolymers display unique reversible mechanical properties owing to the breaking and recovering of the intramolecular hydrogen bonds. When the folded segments are incorporated into the dumbbell components of the donor–acceptor interaction-based pseudo[2]rotaxanes and [2]rotaxanes, they are capable of tuning the slippage/deslippage and switching of the ring component between the discrete "stations" in their dumbbell component.

Keywords: copolymers; foldamers; hydrogen bonds; macrocyclization; rotaxanes.

INTRODUCTION

Nature utilizes about 20 aliphatic α-amino acids to build the backbones of peptides and proteins and the intramolecular N–H···O=C hydrogen bonding of the amide segments to stabilize their secondary and higher-grade structures. As a result, natural peptides and proteins can exhibit many advanced functions which are life-sustaining. In the past decade, chemists have designed many unnatural β-, γ-, δ-amino acids and other similar segments to create artificial secondary structures, which have found various applications in drug design and research in chemical biology [1]. Although several natural α-amino acids bear aromatic units on their side chains, peptides and proteins that contain aromatic amino acid units in the backbones are rare. Compared to the aliphatic counterparts, aromatic amide units possess

Pure Appl. Chem.* **84, 861–1112 (2012). A collection of invited papers based on presentations at the 14th International Symposium on Novel Aromatic Compounds (ISNA-14), Eugene, OR, USA, 24–29 July 2011.
‡Corresponding author: E-mail: ztli@fudan.edu.cn

increased stability, planarity, and conformational predictability. Therefore, in recent years, artificial secondary structures that consist of aromatic amide units have also received great attention [2]. Since aromatic amides themselves can only form intermolecular N–H···O=C hydrogen bonding [3], discrete hydrogen-bonding acceptors have to be introduced to the *ortho*-positions of the amide units to give rise to stable intramolecular hydrogen bonding and also to inhibit competing intermolecular hydrogen bonding [2a–c]. Continual intramolecular hydrogen bonds of this nature can induce the linear backbones to generate compact conformations of the lowest energy. By controlling the positions of the amides and substituents on the aromatic rings in oligomeric backbones, we are able to generate discrete conformations or shapes, including folded/helical, straight, or zigzag shapes, if the backbones are long enough.

Our effort in developing aromatic amide-based foldamers started in 2002. In 2004, we reported our first class of aromatic foldamers (**1a–c**), which consist of aromatic hydrazide-based backbones [4]. In the following years, we also developed several classes of aromatic amide-based foldamers (**2–6**) that have folded (**2–4**) [5–7], straightforward (**5a–c**) [8], and zigzag (**6a–d**) [9] conformations. An extensive investigation of the structure–property relationship of the foldamers was then carried out [2f,g]. Throughout the effort, we have explored many applications of this family of preorganized aromatic frameworks, including developing folded receptors and molecular tweezers [10,11], assembling two- or three-dimensional ordered architectures such as homoduplexes [12], nano networks [13], vesicles and organogels [14], and liquid crystals [15], accelerating the hydrolysis of ethers [10b], regulating the intramolecular electron transfer [16], promoting macrocyclization [17,18], tuning the aggregation, thermal and mechanical property of polymers and copolymers [19], and modulating the slippage/deslippage and switching of the ring component over the dumbbell component of pseudorotaxanes and rotaxanes [20]. In this report, we discuss the three latter topics, which have attracted our attention during recent years.

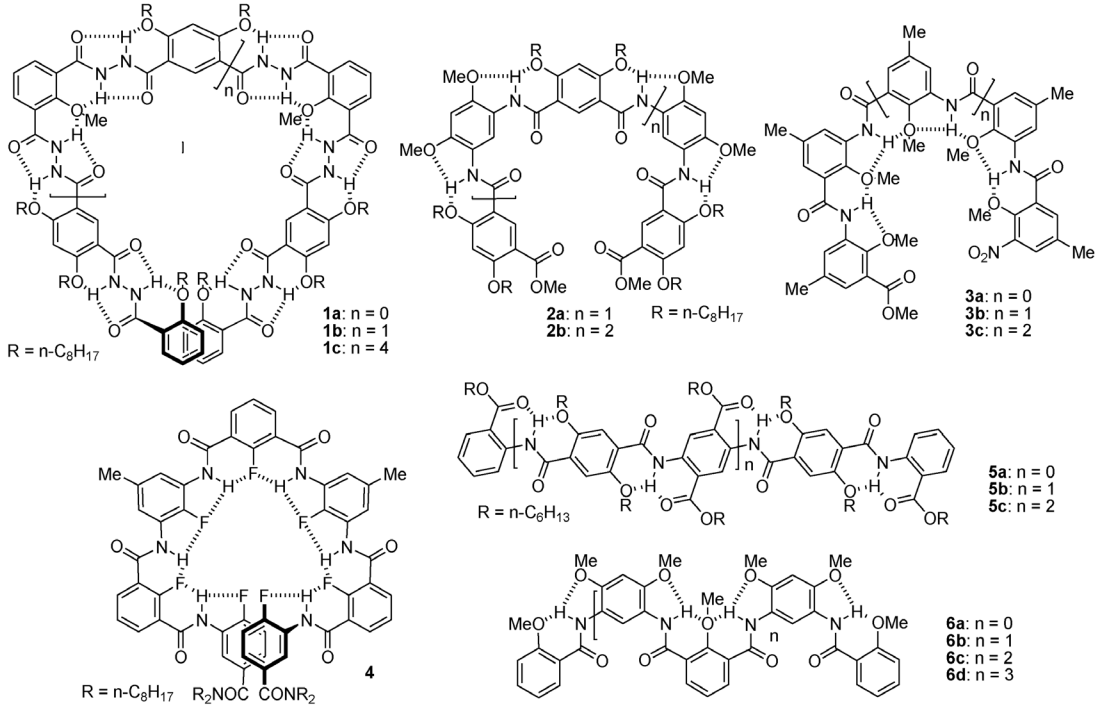

PROMOTION OF MACROCYCLIZATION

The development of efficient methods for the syntheses of macrocycles has been a challenge in organic synthesis owing to competitively favored formation of linear byproducts [21]. The preorganized conformation of hydrogen-bonded aromatic oligomers can be utilized to promote the selective formation of macrocyclic structures [2g]. By using this principle, we have constructed several large metallocyclophanes through the formation of the coordination bonds [17a,b]. For example, metallomacrocycles **7a,b** can be obtained in 18–20 % yields from the reactions of the related hydrogen-bonded precursors and $PtCl_2(Ph_2PCH_2CH_2PPh_2)$. Although the yields are modest, control experiments showed that similar macrocyclic products could not be separated when hydrogen bonding-free precursors of the same backbones were used.

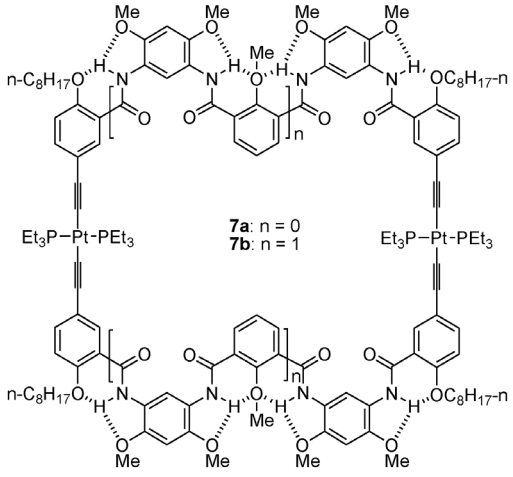

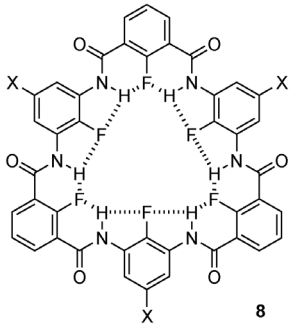

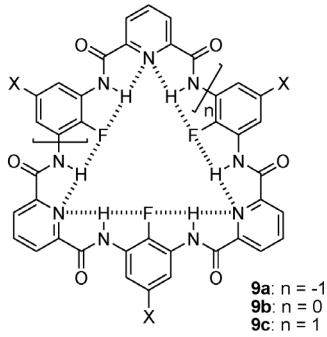

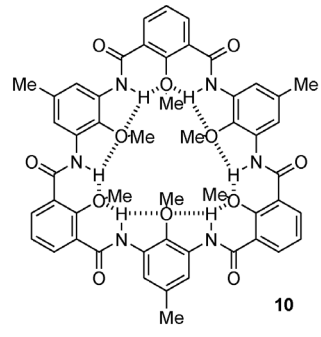

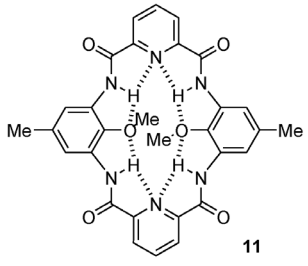

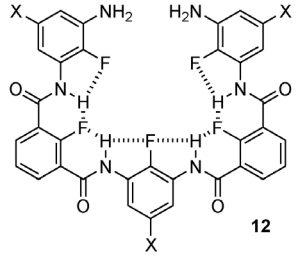

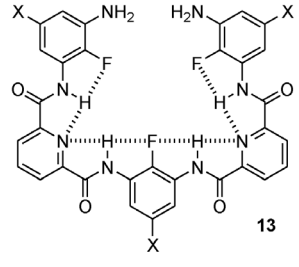

X = CO(n-C8H17)2

The formation of the amide bonds for the cyclization step has received more attention [22]. For example, by using this approach, Gong and co-workers reported that amide macrocycles could be obtained in as high as 69–82 % yields from the one-pot reactions of simple diacyl chlorides and diamines [22a,b]. For all their reactions, the substituents that form the designed intramolecular hydrogen bonding are positioned from outside the macrocycles. We found that, when the groups that form intramolecular hydrogen bonds are orientated inwards the designed macrocycles, similar one-pot reactions from simple diacyl chloride and diamine precursors afforded macrocycles of different sizes [17c]. Thus, 6-mer macrocycles **8** and **10** and 4-mer macrocycle **11** were selectively formed in 40–45 % yields from the corresponding diacyl chlorides and diamines, while 2-, 4-, and 6-mer cycles **9a–c**, which were separated by column chromatography, were generated in 80 % total yield from another similar reaction. These results show that the geometric feature of the precursors has an important effect on the cyclization selectivity. For comparison, the step-by-step approach was also investigated, and treatment of pentamers **12** and **13** with the related diacyl chlorides under the same reaction conditions gave rise to **8** and **9c** in 55 and 54 % yields, respectively.

Hydrogen bonding-induced preorganization of precursors also facilitates the generation of macrocycles through the formation of the triazole. For example, the click reaction of U-shaped **14** and **15** in chloroform in the presence of CuI and *N*,*N*-diisopropylethylamine (DIPEA) afforded macrocycle **16** in 82 % yield (Scheme 1) [17d]. By using the same approach, macrocycles **17–19** can be prepared in 85, 20, and 25 % yields, respectively, from the corresponding diazide and diacetylene precursors. The low yield of the smallest macrocycle **18** indicates that its short but straight bisazide precursor was not as efficient as the longer but "U"-shaped precursors of other macrocycles in forming the cyclic structure, confirming the importance of the preorganization in promoting macrocyclization.

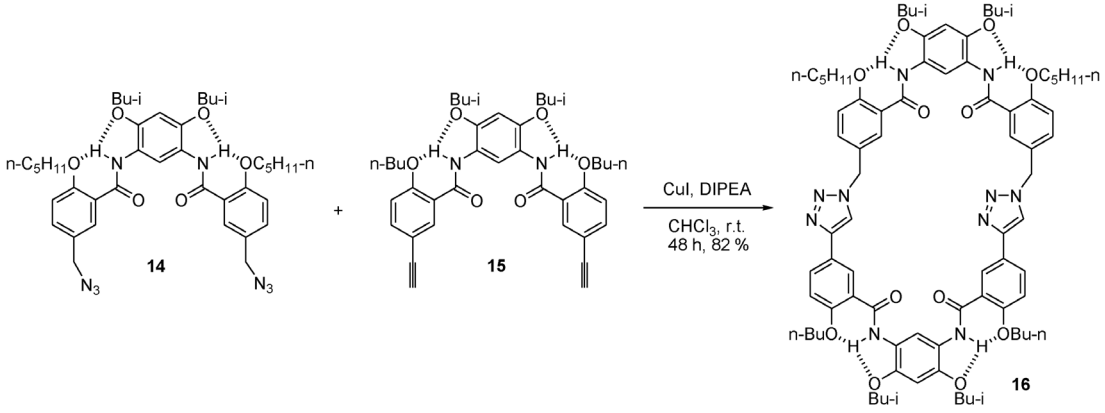

Scheme 1 Synthesis of macrocycle **16** from preorganized precursors **14** and **15**.

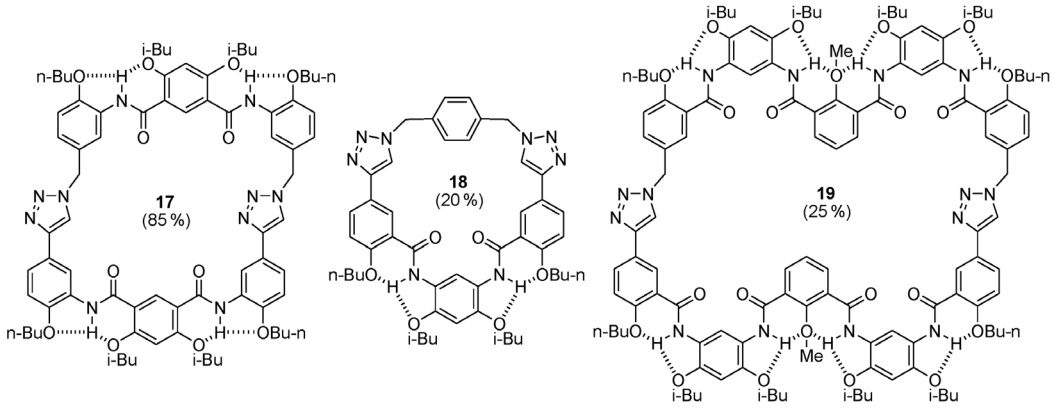

The above results clearly show that hydrogen bonding-induced preorganization of the precursors and intermediates works well in promoting macrocyclization. However, the intrinsic feature of the dynamic control of these reactions makes it impossible to avoid the competitive formation of linear byproducts. Therefore, we have also pursued the dynamic covalent chemistry (DCC) approach to achieve even higher macrocyclization yields [23]. DCC has been demonstrated to be robust in the construction of complicated macrocyclic architectures [24]. To test the efficiency of this approach, we first prepared hydrogen-bonded U-shaped precursors **20** and **21** [18a]. The ^{1}H NMR spectrum showed that, after reaching an equilibrium, their 1:1 mixture (2.5 mM) in $CDCl_3$/DMSO-d_6 (4:1) afforded macrocycle **22** exclusively (≥95 %), without removing the water formed in the reaction (Scheme 2). The X-ray structures of precursors **20** and **21** revealed that the distances between their aldehyde and amino groups were very close, which made the formation of macrocycle **22** much more favorable than any other cyclic or linear products. The X-ray structure of **22** also showed that macrocyclization did not substantially change the conformation of the two components, implying that the intramolecular hydrogen bonds were still able to stabilize the cyclic structure.

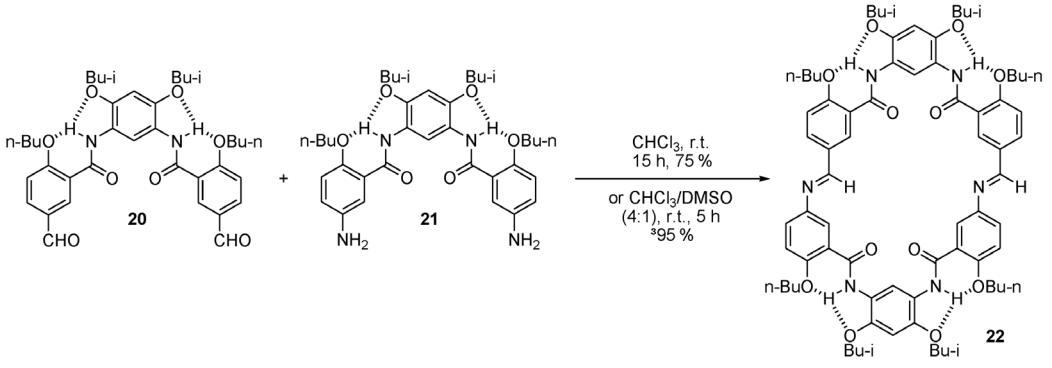

Scheme 2 Synthesis of macrocycle **22** from preorganized precursors **20** and **21**.

Encouraged by the above results, we also prepared compound **23**. The aldehyde and amino units of this precursor were designed to orientate at around 60º for the formation of the macrocyclic architecture from three identical segments [18c]. In the presence of trifluoroacetic acid (TFA), **23** self-coupled in chloroform to give macrocycle **24** selectively (Scheme 3). In the same way, hydrazone-based macrocycles could also be prepared quantitatively from the corresponding precursor. To further expand the scope of this approach, we also prepared dipodal precursors **25a–c** [18c]. Treatment of these precursors with TFA in chloroform led to the formation of two-layered capsules **26a–c** in 82 to 100 % yields (Scheme 3). Compounds **26a,b** can bind linear diammonium derivatives in chloroform to give rise to new pseudo[3]rotaxanes which are stabilized by the intermolecular N–H···O=C hydrogen bonding between the ammonium protons and the carbonyl oxygen atoms.

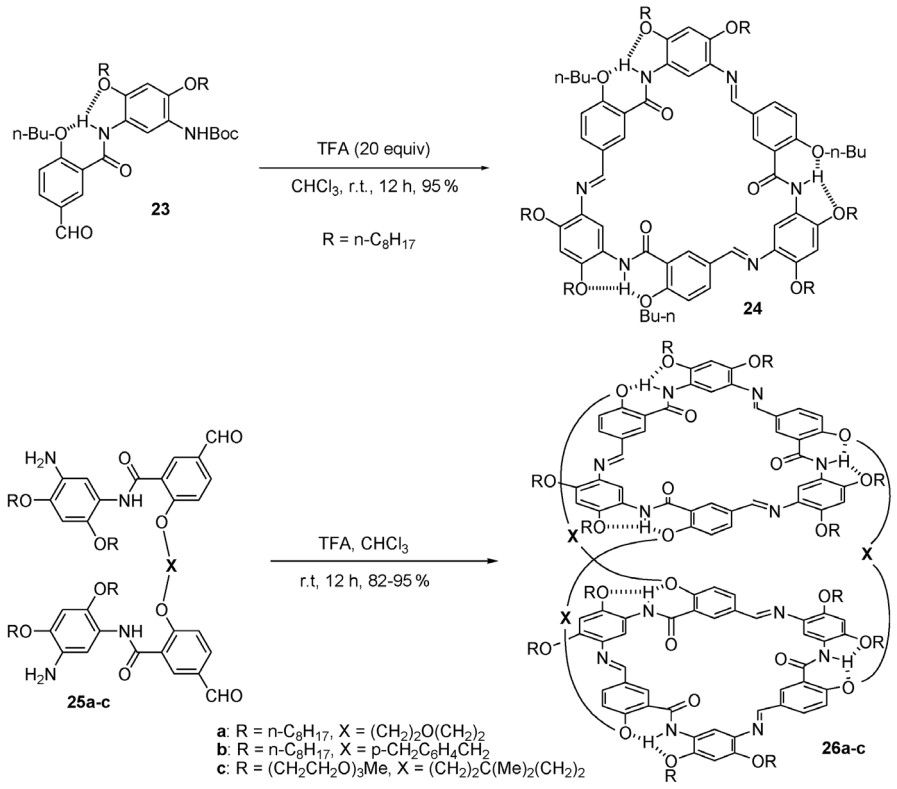

Scheme 3 Synthetic routes for macrocycle **24** and two-layered capsules **26a–c**.

Macrocycle **27** could also be formed selectively from four precursors through the formation of four imine bonds, while bimacrocycle **28** could be generated from six precursors through the formation of seven imine bonds [18a]. By using the similar approach, macrocycles **29a–c** have also been prepared from the corresponding di-, tri, and tetraamines and terephthalaldehyde through the formation of four, six, or eight imine bonds [18b]. All the macrocyclic compounds could be purified by simple filtration. Compounds **28** and **29a–c** are soluble in chloroform, but their ^{1}H NMR spectra in $CDCl_3$ or DMSO-d_6 are of low resolution, reflecting that strong intermolecular stacking occurs owing to the rigidity of the backbones. Also under the direction of the intramolecular hydrogen bonding, cyclotriveratrylene (CTV)-based capsules **30a,b** could also be assembled quantitatively from the corresponding C_3-symmetric CTV precursors by forming three imine bonds from arylamide-derived foldamer segments [18d].

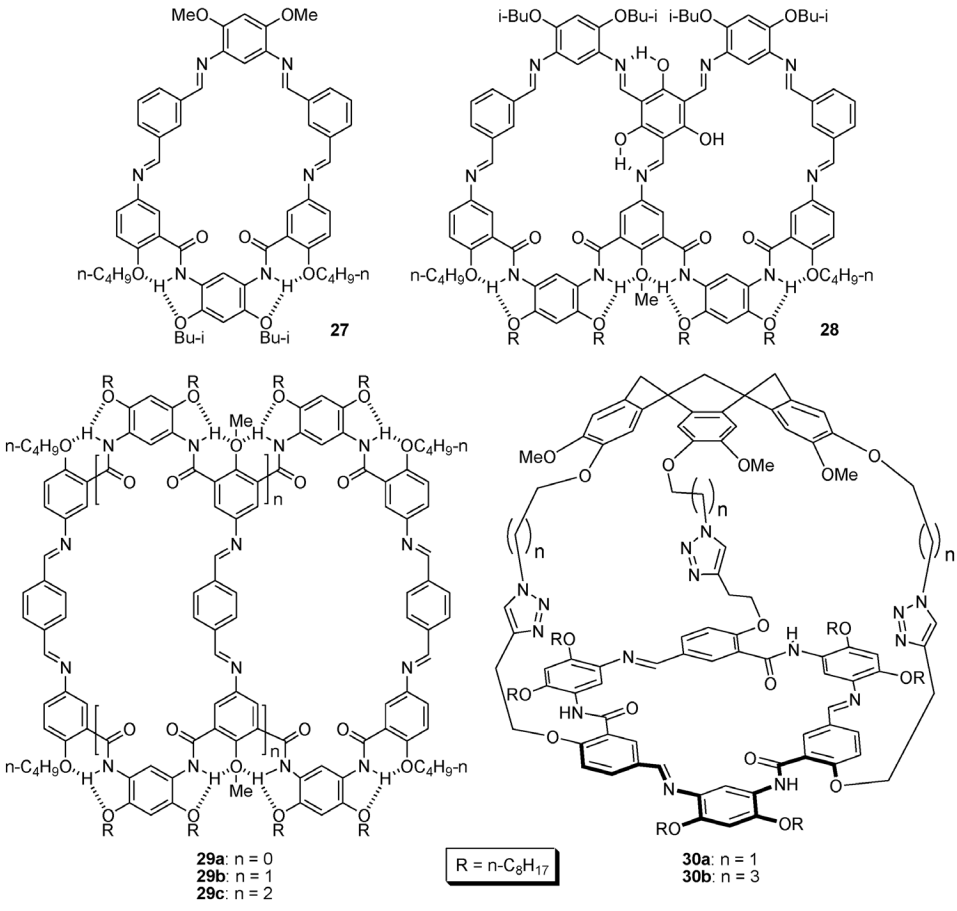

^{1}H and ^{13}C NMR and UV/vis experiments revealed that the two capsular compounds encapsulated C_{60} and C_{70} to form stable 1:1 complexes in discrete solvents. Macrocycles **24** and **26a** could be quantitatively reduced with $NaHB(CN)_3$ to the corresponding triamine and hexamine derivative [14e]. These amines could be further methylated with methyl iodide to afford the corresponding ammoniums. These ammonium mono- and bi-layered macrocycles, as iodide salts, could form reverse vesicles in chloroform. With large perchloride as the anion, the corresponding salts did not form vesicles, and the ammonium monomacrocycle that bears larger ethyl groups did not either. These results suggested that the stacking of the large cationic macrocycles played a key role for the formation of the reverse vesicles.

PREORGANIZED HYDRAZIDE POLYMERS

The concept of hydrogen bonding-driven preorganization can also be extended to polymeric backbones [19a]. We have prepared hydrazide-based zigzag polymers **P31a–e** from the corresponding 4,6-dialkoxyisophthalic acid and 4,6-dialkoxyisophthalohydrazide precursors by using the Yamazaki polymerization conditions [25]. The hydrazine backbones were expected to adopt an extended conformation owing to the continual intramolecular hydrogen bonds and the intrinsic rigidity of the hydrazide units, while the hydrophobic, hydrophilic, or amphiphilic side chains were attached to the extended backbones to tune their solubility in organic solvents of different polarity. Scanning electron microscopy (SEM) and transmission electron microscopy (TEM) experiments revealed that the new shape-persistent polymers self-assembled into vesicles or fibrous structures to gelate organic solvents

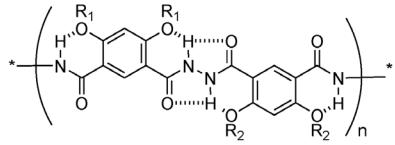

P31a: $R_1 = R_2 = n\text{-}C_{12}H_{25}$
P31b: $R_1 = n\text{-}C_{12}H_{25}$, $R_2 = (CH_2CH_2O)_3Me$
P31c: $R_1 = R_2 = CH_2CONHCH_2CON(n\text{-}C_8H_{17})_2$
P31d: $R_1 = CH_2CONHCH_2CON(n\text{-}C_8H_{17})_2$, $R_2 = Me$
P31e: $R_1 = R_2 = (CH_2CH_2O)_3Me$

of different polarity. Control experiments showed that short hydrazide molecules did not form similar ordered architectures. Thus, the formation of the ordered supramolecular architectures by these hydrogen-bonded rigid polymers was attributed to the increased stacking of their hydrazide backbones. This class of hydrogen-bonded polymeric backbones may be regarded as a conceptual extension of foldamers, which are usually constructed from oligomeric backbones.

TUNING THE THERMAL AND MECHANICAL PROPERTY OF COPOLYMERS

Cross-linked methacrylate (co)polymers are a family of thermo-set elastomers that have many industrial applications. Conventional cross-links consist of various covalently bonded flexible or rigid chains. These cross-links may display conformational or shape change upon stressing or heat. However, the cross-links usually do not have additional intramolecular interactions that are consumed owing to a conformational change. In searching for new tunable and reversibly dissipative cross-linking modes, we have prepared a series of aromatic amide-based folded segments **HB32-**nm (n = 1, 3, 5) [19b]. These diamines were reacted with salicylaldehyde-bearing prepolymer **PP33** to form cross-linked copolymers **HB34**-nP (n = 1, 3, 5). As controls, we also prepared analogous aromatic cross-links **NB32**-nm (n = 1, 3, 5), which were not able to generate the folded structures owing to the lack of the specific intramolecular hydrogen bonding, to prepare copolymers **NB34**-nP under the identical reaction conditions. From the two series of cross-linked copolymers, we prepared 18 films of the same thickness and size and systematically investigated their dynamic mechanical and creep/stress relaxation (recovery) properties. It was revealed that, compared to the control copolymers, the hydrogen-bonded foldamer cross-links substantially improved the mechanical properties of the copolymers. The result was attributed to the ability of the folded cross-links to reversibly reveal the hidden length on extension via dissipative cleavage of their intramolecular hydrogen bonding, as shown in Fig. 1.

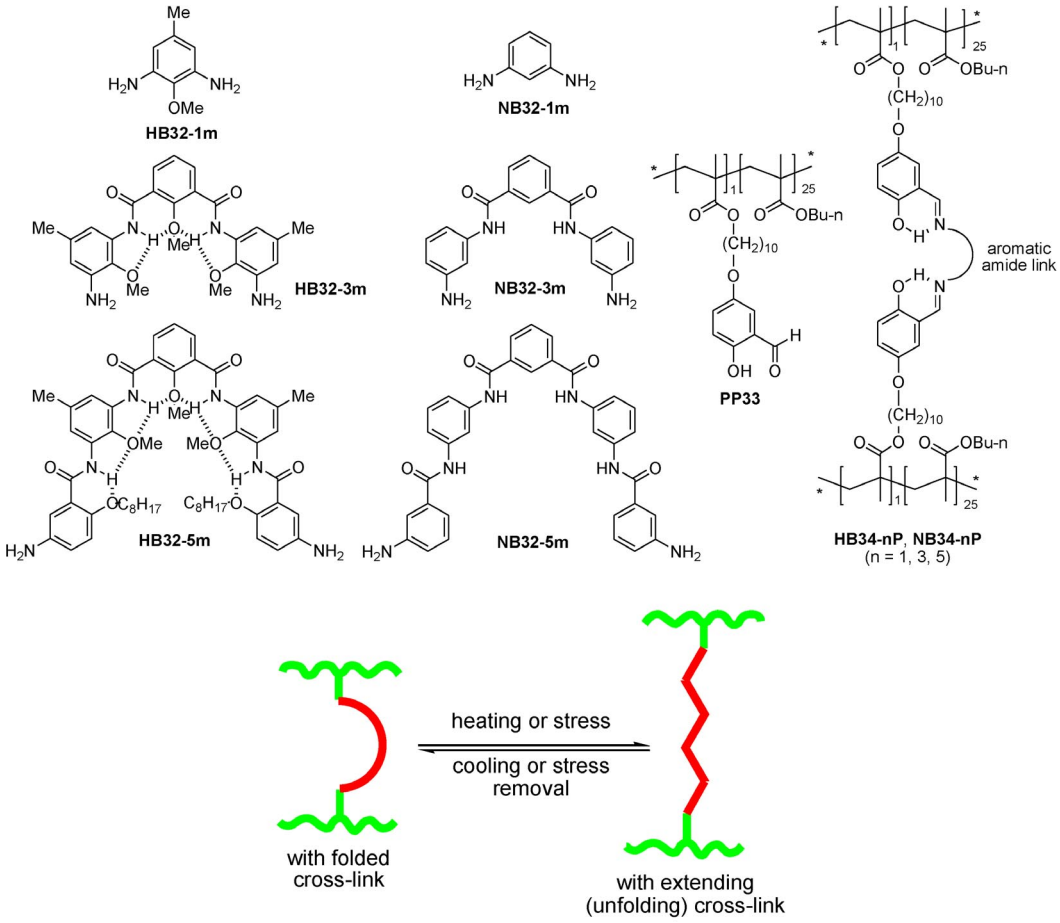

Fig. 1 Schematic representation of the hydrogen-bonded foldamer cross-links in *n*-butyl methacrylate copolymers. Heating or applying a stress causes the folded state to unfold or extend, while cooling or removing the stress results in the recovery of the folded state.

FOLDAMERS FOR TUNING SWITCHING KINETICS AND METASTABILITY OF PSEUDO[2]ROTAXANES AND [2]ROTAXANES

Rotaxane-based molecular switches and devices have been the topic of extensive investigations in supramolecular chemistry [26]. In this context, bistable [2]rotaxanes, consisting of a linear component incorporated with electron-rich tetrathiafuvalene (TTF) and 1,5-dioxynaphthalene (DNP) binding sites which is encircled by a cyclobis-(paraquat-*p*-phenylene) ($CBPQT^{4+}$) ring, have been investigated as devices for high-density molecular memories [27]. One issue associated with bistable [2]rotaxane-related devices is the short lifetime of their metastable-state co-conformation (MSCC) owing to its quick relaxation to the ground-state co-conformation (GSCC) [28]. It has been demonstrated that introducing a bulky or electrostatic barrier between the TTF and DNP units can slow down the back-shuttling of the $CBPQT^{4+}$ ring from the DNP unit to the neutral TTF unit and thus generate long-lived MSCC even after removal of the bias by rapid reduction of the pre-oxidized TTF unit [29]. However, it is still a challenge to develop novel strategies for controlling the interconversion between the GSCC and the MSCC in a modular manner.

We recently reported that hydrogen bonding-mediated aromatic amide foldamers could be utilized to tune this interconversion [20]. The new approach is based on the fact that a folded state has an apparent size larger than that of an extended one. When the apparent diameter of the extended state of a foldamer is smaller than the internal diameter of a macrocycle, while the diameter of its folded state is larger, it is expected that the macrocycle will be able to slip over the extended state. However, the process would be decelerated compared with that over a similar but flexible molecule, because it needs to, at least partially, break the noncovalent bonds existing in the folded state as shown in Fig. 2.

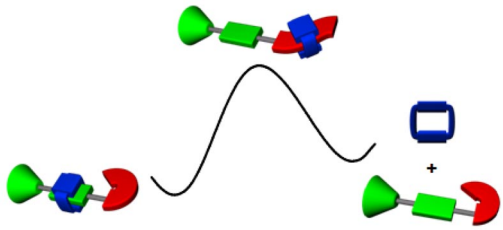

Fig. 2 Schematic representation depicting the foldamer-modulated extrusion (pseudo[2]rotaxane decomplexation) or slippage (pseudo[2]rotaxane formation) of the $CBPQT^{4+}$ ring from or onto a TTF-containing thread. The foldamer segment in its folded state has a large apparent size and must unfold into an extended conformation to allow for the passing of the $CBPQT^{4+}$ ring.

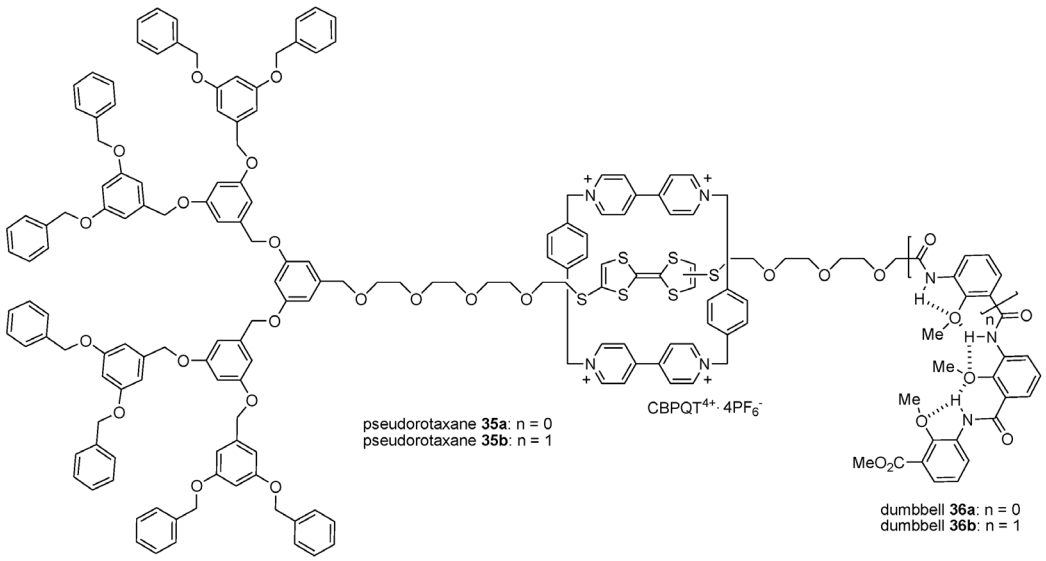

Pseudo[2]rotaxanes **35a,b** were assembled, respectively, from dumbbells **36a,b** and $CBPQT^{4+}$ hexafluorophosphate and purified by making use of the solubility difference of the three species. The large dendron provided good solubility for the pseudo[2]rotaxanes in different solvents [30]. The pseudo[2]rotaxanes decomposed in polar solvents like acetonitrile and dimethyl sulfoxide (DMSO), but the stability of the pseudo[2]rotaxanes as complexes was comparable to that of the model donor–acceptor complex, indicating that the foldamer segment in the dumbbells did not impose an important effect on the donor–acceptor interaction between the TTF unit of the dumbbell and the $CBPQT^{4+}$ ring. The kinetics of extrusion of the $CBPQT^{4+}$ ring from the dumbbell of **35a,b** was investigated using the UV–vis spectroscopy with the TTF-$CBPQT^{4+}$ charge-transfer (CT) absorption as

the probe. The rate constants (k_{off}) of the extrusion of the tetracationic ring from the dumbbells in solvents of both low and high polarity were derived by assuming first-order kinetics. The data, together with the associated changes of free energy, are provided in Table 1. The largest k_{off} was displayed by **35a** in polar dimethyl formamide (DMF), which corresponded to a half-life of 301 s, while the slowest one was displayed by **35b** in chloroform, which corresponded to a half-life of 67 days. The two data had a difference of as high as 19 167 times. Thus, by choosing discrete foldamer segments and media, we could regulate the passing of the CBPQT^{4+} ring from the foldamer segments in a remarkably long span of time.

Table 1 The kinetic data for the extrusion of the CBPQT^{4+} ring over the foldamer segments in pseudo-[2]rotaxanes **35a,b** at 25 °C in different solvents.

Solvent	ε^a	**35a**		**35b**	
		k_{off} (s^{-1})	$\Delta G^{\neq}$ ($kJ \cdot mol^{-1}$)	k_{off} (s^{-1})	$\Delta G^{\neq}$ ($kJ \cdot mol^{-1}$)
DMSO	47.2	1.0×10^{-3}	90	1.1×10^{-4}	96
DMF	36.7	2.3×10^{-3}	88	4.7×10^{-4}	92
MeCN	38.3	5.2×10^{-4}	92	4.0×10^{-5}	98
PhCN	25.7	2.8×10^{-4}	93	2.0×10^{-5}	100
Acetone	21.0	8.4×10^{-4}	91	1.3×10^{-4}	95
$Cl(CH_2)_2Cl$	10.4	7.5×10^{-6}	102	2.0×10^{-7}	111
THF	7.5	2.6×10^{-4}	94	8.3×10^{-6}	102
Chloroform	4.8	1.9×10^{-6}	106	1.2×10^{-7}	113

[a]Dielectric constant of the solvent.

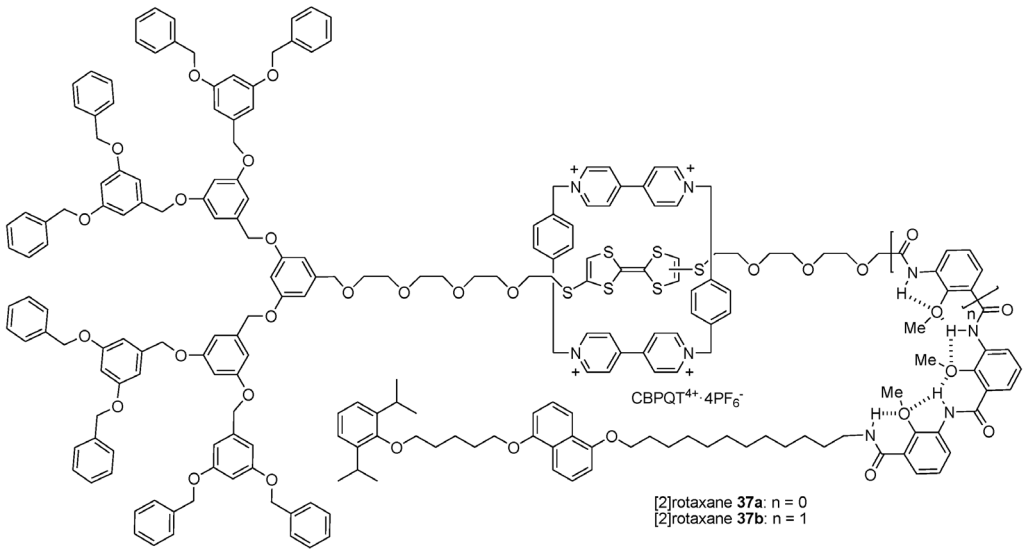

Since the dimeric and trimeric foldamer segments in pseudo[2]rotaxanes **35a,b** could provide an energy barrier for the CBPQT^{4+} ring to extrude at a rate of 10^{-3}~10^{-7} s^{-1}, we further prepared bistable [2]rotaxanes **37a,b** to study the switching of the CBPQT^{4+} ring between the TTF and DNP sites over the foldamer segment [20]. Because the TTF unit is more electron-rich than the DNP unit, in a two-state model (Fig. 3), we expected the equilibrium to shift toward the CBPQT^{4+} ring encircling the TTF site

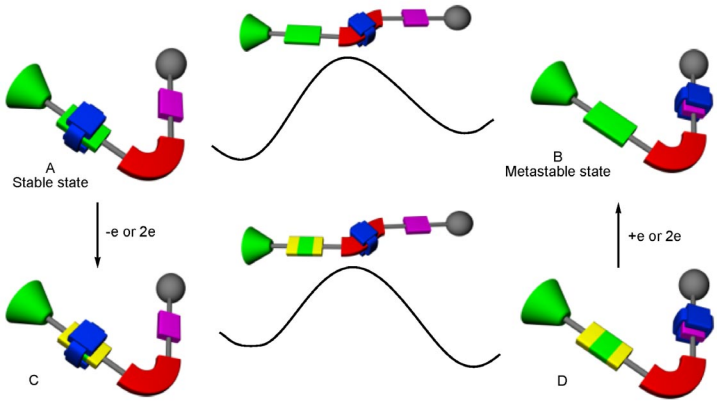

Fig. 3 Schematic representation depicting the foldamer-tuned switching of the $CBPQT^{4+}$ ring between the TTF and DNP sites in bistable [2]rotaxanes **37a,b**, with the TTF unit being neutral or oxidized to $TTF^{+\cdot}$ or TTF^{2+}.

to form the GSCC, rather than toward the $CBPQT^{4+}$ ring encircling the DNP site to form the less stable MSCC. The ^1H NMR spectra of [2]rotaxanes **37a,b** in acetonitrile-d_3 and acetone-d_6 displayed one set of signals, indicating that their $CBPQT^{4+}$ ring did predominantly encircle the TTF unit to form the GSCC (A, Fig. 3). Oxidizing the TTF unit to $TTF^{+\cdot}$ or TTF^{2+} with $Fe(ClO_4)_3$ or Magic Blue [$(4\text{-}BrC_6H_4)_4N^+SbCl_6^-$] forced the $CBPQT^{4+}$ ring to shift to encircle the DNP unit. Upon the oxidized TTF unit being reduced to the neutral one with an excess of zinc powder, the $CBPQT^{4+}$ ring was induced to shift back to the TTF site again. These processes were confirmed by ^1H NMR and UV–vis experiments.

The time-dependent UV–vis spectra of the as-reduced solutions of the bistable [2]rotaxanes showed that the DNP-$CBPQT^{4+}$ CT absorption at 550 nm gradually decreased, while the TTF-$CBPQT^{4+}$ CT absorption at 805 nm appeared and increased gradually. By assuming first-order kinetics, we determined the rate constants of the shuttling of the $CBPQT^{4+}$ ring of **37a,b** from the MSCC to the GSCC (B $\rightarrow$ A, Fig. 3) to be 1.1×10^{-2} and 7.4×10^{-4} s^{-1}, respectively, which corresponded to half-lives of 66 and 930 s. By using the same method, we determined the rate constant of the same process of **37a** in chloroform to be 9.9×10^{-6} s^{-1}, which corresponded to a half-life of 19.5 h, 1064 times longer than that of **37a** in acetonitrile. These rate constants were all higher than the related k_{off} values of pseudorotaxanes **35a,b**, which was consistent with the fact that the donor–acceptor interaction between the DNP unit and $CBPQT^{4+}$ was weaker than that between the TTF unit and the $CBPQT^{4+}$ ring. Remarkably, the solution of the MSCC of **37b** in chloroform did not exhibit a perceptible TTF-$CBPQT^{4+}$ CT band in the UV–vis spectrum even after three days, indicating that the foldamer segment efficiently blocked the conversion of the MSCC to the GSCC in this less polar solvent. Because both bistable [2]rotaxanes are soluble in organic solvents of both low and high polarity, the results suggest that, by changing the length of the foldamer segments and the polarity of the media, we are able to control the lifetime of the MSCC of the [2]rotaxanes in a large time scale.

CONCLUSION

The studies described in this report demonstrates that hydrogen-bonded aromatic amide foldamers represent a new family of preorganized soft frameworks which can be used in quite a number of different research areas. The functional diversity of this family of foldamers comes from their structural diversity as a result of varying hydrogen-bonding patterns, aromatic segments, backbone shape and length, and attached side chains. It is expected that new hydrogen-bonding patterns and frameworks should be developed in the coming years. Helical or extended polymeric backbones may be created, which may find applications in developing one-dimensional nano and template materials and polyelectrolytes as

well as electronic materials, if conjugated units are introduced to one or two sides of the backbones. The potential of the rigid macrocycles, which can be quickly constructed by using the DCC approach, as molecular receptors have not been exploited. The possibility of incorporating the foldamer segment into catenanes is also worth studying. Thus, new exciting advances may be expected in the future.

ACKNOWLEDGMENTS

We are grateful to the National Natural Science Foundation of China (Nos. 20921091, 20732007, 20974118, and 20872167), Ministry of Science and Technology of China (2007CB-808001), and Science and Technology Commission of Shanghai Municipality (09XD1405300) for financial support. ZTL also thank his able graduates at Shanghai Institute of Organic Chemistry and collaborators, whose names are cited in the references, for their contributions.

REFERENCES

1. S. Hecht, I. Huc (Eds). *Foldamers: Structure, Properties and Applications*, Wiley-VCH, Weinheim (2007).
2. (a) B. Gong. *Chem.—Eur. J.* **7**, 4336 (2001); (b) I. Huc. *Eur. J. Org. Chem.* 17 (2004); (c) Z.-T. Li, J.-L. Hou, C. Li, H.-P. Yi. *Chem. Asian J.* **1**, 766 (2006); (d) B. Gong. *Acc. Chem. Res.* **41**, 1376 (2008); (e) I. Saraogi, A. D. Hamilton. *Chem. Soc. Rev.* **38**, 1726 (2009); (f) Z.-T. Li, J.-L. Hou, C. Li. *Acc. Chem. Res.* **41**, 1343 (2008); (g) X. Zhao, Z.-T. Li. *Chem. Commun.* **46**, 1601 (2010); (h) G. Guichard, I. Huc. *Chem. Commun.* **47**, 5933 (2011); (i) Q. Gan, Y. Wang, H. Jiang. *Curr. Org. Chem.* **15**, 1293 (2011); (j) Y.-Y. Zhu, G.-T. Wang, Z.-T. Li. *Curr. Org. Chem.* **15**, 1266 (2011); (k) Z.-T. Li. *Huaxue Jinzhan* **23**, 1 (2011).
3. D. Tanner, J. A. Fitzgerald, B. R. Phillips. *Angew. Chem., Int. Ed. Engl.* **28**, 649 (1989).
4. J.-L. Hou, X.-B. Shao, G.-J. Chen, Y.-X. Zhou, X.-K. Jiang, Z.-T. Li. *J. Am. Chem. Soc.* **126**, 12386 (2004).
5. C. Li, S.-F. Ren, J.-L. Hou, H.-P. Yi, S.-Z. Zhu, X.-K. Jiang, Z.-T. Li. *Angew. Chem., Int. Ed.* **44**, 5725 (2005).
6. H.-P. Yi, X.-B. Shao, J.-L. Hou, C. Li, X.-K. Jiang, Z.-T. Li. *New J. Chem.* **29**, 1213 (2005).
7. H.-P. Yi, C. Li, J.-L. Hou, X.-K. Jiang, Z.-T. Li. *Tetrahedron* **61**, 7974 (2005).
8. Z.-Q. Wu, X.-K. Jiang, S.-Z. Zhu, Z.-T. Li. *Org. Lett.* **6**, 229 (2004).
9. J. Zhu, X.-Z. Wang X.-B. Shao, J.-L. Hou, X.-Z. Chen, X.-K. Jiang, Z.-T. Li. *J. Org. Chem.* **69**, 6221 (2004).
10. (a) C. Li, G.-T. Wang, H.-P. Yi, X.-K. Jiang, Z.-T. Li, R.-X. Wang. *Org. Lett.* **9**, 1797 (2007); (b) H.-P. Yi, J. Wu, K.-L. Ding, X.-K. Jiang, Z.-T. Li. *J. Org. Chem.* **72**, 870 (2007); (c) Y.-X. Xu, X. Zhao, X.-K. Jiang, Z.-T. Li. *J. Org. Chem.* **74**, 7267 (2009); (d) P. Du, Y.-X. Xu, X.-K. Jiang, Z.-T. Li. *Sci. China, Ser. B* **52**, 489 (2009).
11. (a) Z.-Q. Wu, X.-B. Shao, C. Li, J.-L. Hou, K. Wang, X.-K. Jiang, Z.-T. Li. *J. Am. Chem. Soc.* **127**, 17460 (2005); (b) Z.-Q. Wu, C.-Z. Li, D.-J. Feng, X.-K. Jiang, Z.-T. Li. *Tetrahedron* **62**, 11054 (2006); (c) J.-L. Hou, H.-P. Yi, X.-B. Shao, C. Li, Z.-Q. Wu, X.-K. Jiang, L.-Z. Wu, C.-H. Tung, Z.-T. Li. *Angew. Chem., Int. Ed.* **45**, 796 (2006); (d) C.-Z. Li, J. Zhu, Z.-Q. Wu, J.-L. Hou, C. Li, X.-B. Shao, X.-K. Jiang, Z.-T. Li, X. Gao, Q.-R. Wang. *Tetrahedron* **62**, 6973 (2006); (e) H. Liu, J. Wu, X.-K. Jiang, Z.-T. Li. *Tetrahedron Lett.* **48**, 7327 (2007); (f) D.-J. Feng, G.-T. Wang, J. Wu, R.-X. Wang, Z.-T. Li. *Tetrahedron Lett.* **48**, 6181 (2007); (g) C.-Z. Li, Z.-T. Li, X. Gao, Q.-R. Wang. *Chin. J. Chem.* **25**, 1417 (2007); (h) J. Wu, J.-L. Hou, C. Li, Z.-Q. Wu, X.-K. Jiang, Z.-T. Li, Y.-H. Yu. *J. Org. Chem.* **72**, 2897 (2007).
12. (a) J. Zhu, J.-B. Lin, Y.-X. Xu, X.-B. Shao, X.-K. Jiang, Z.-T. Li. *J. Am. Chem. Soc.* **128**, 12307 (2006); (b) J. Zhu, J.-B. Lin, Y.-X. Xu, X.-K. Jiang, Z.-T. Li. *Tetrahedron* **62**, 11933 (2006).
13. C. Li, Y.-Y. Zhu, H.-P. Yi, C.-Z. Li, X.-K. Jiang, Z.-T. Li. *Chem.—Eur. J.* **13**, 9990 (2007).

14. (a) W. Cai, G.-T. Wang, Y.-X. Xu, X.-K. Jiang, Z.-T. Li. *J. Am. Chem. Soc.* **130**, 6936 (2008); (b) W. Cai, G.-T. Wang, P. Du, R.-X. Wang, X.-K. Jiang, Z.-T. Li. *J. Am. Chem. Soc.* **130**, 13450 (2008); (c) L. Wang, Z.-Y. Xiao, J.-L. Hou, G.-T. Wang, X.-K. Jiang, Z.-T. Li. *Tetrahedron* **65**, 10544 (2009); (d) L.-Y. You, X.-K. Jiang, Z.-T. Li. *Tetrahedron* **65**, 9494 (2009); (e) X.-N. Xu, L. Wang, Z.-T. Li. *Chem. Commun.* 6634 (2009); (f) B.-Y. Lu, J.-B. Lin, X.-K. Jiang, Z.-T. Li. *Tetrahedron Lett.* **51**, 3830 (2010); (g) J.-B. Lin, G.-T. Wang, X.-K. Jiang, Z.-T. Li. *Tetrahedron Lett.* **51**, 4221 (2010).
15. (a) Z.-Y. Xiao, J.-L. Hou, X.-K. Jiang, Z.-T. Li, Z. Ma. *Tetrahedron* **65**, 10182 (2009); (b) G.-T. Wang, X. Zhao, Z.-T. Li. *Tetrahedron* **67**, 48 (2011).
16. K. Wang, Y.-S. Wu, G.-T. Wang, R.-X. Wang, X.-K. Jiang, H.-B. Fu, Z.-T. Li. *Tetrahedron* **65**, 7718 (2009).
17. (a) Y.-Q. Chen, X.-Z. Wang, X.-B. Shao, J.-L. Hou, X.-Z. Chen, X.-K. Jiang, Z.-T. Li. *Tetrahedron* **60**, 10253 (2004); (b) Z.-Q. Wu, X.-K. Jiang, Z.-T. Li. *Tetrahedron Lett.* **46**, 8067 (2005); (c) Y.-Y. Zhu, C. Li, G.-Y. Li, X.-K. Jiang, Z.-T. Li. *J. Org. Chem.* **73**, 1745 (2008); (d) Y.-Y. Zhu, G.-T. Wang, Z.-T. Li. *Org. Biomol. Chem.* **7**, 3243 (2009).
18. (a) J.-B. Lin, X.-N. Xu, X.-K. Jiang, Z.-T. Li. *J. Org. Chem.* **73**, 9403 (2008); (b) J.-B. Lin, J. Wu, X.-K. Jiang, Z.-T. Li. *Chin. J. Chem.* **27**, 117 (2009); (c) X.-N. Xu, L. Wang, J.-B. Lin, G.-T. Wang, X.-K. Jiang, Z.-T. Li. *Chem.—Eur. J.* **15**, 5763 (2009); (d) L. Wang, G.-T. Wang, X. Zhao, X.-K. Jiang, Z.-T. Li. *J. Org. Chem*. **76**, 3531 (2011).
19. (a) C. Zhou, W. Cai, G.-T. Wang, X. Zhao, Z.-T. Li. *Macromol. Chem. Phys.* **211**, 2090 (2010); (b) Z.-M. Shi, J. Huang, Z. Ma, Z. Guan, Z.-T. Li. *Macromolecules* **43**, 6185 (2010).
20. K.-D. Zhang, X. Zhao, G.-T. Wang, Y. Liu, Y. Zhang, H.-J. Lu, X.-K. Jiang, Z.-T. Li. *Angew. Chem., Int. Ed.* **50**, 9866 (2011).
21. R. Gleiter, H. Hopf (Eds.). *Modern Cyclophane Chemistry*, Wiley-VCH, Weinheim (2004).
22. (a) L. H. Yuan, W. Feng, K. Yamato, A. R. Sanford, D. G. Xu, H. Guo, B. Gong. *J. Am. Chem. Soc.* **126**, 11120 (2004); (b) W. Feng, K. Yamato, L. Q. Yang, J. S. Ferguson, L. J. Zhong, S. L. Zou, S. L. H. Yuan, X. C. Zeng, B. Gong. *J. Am. Chem. Soc.* **131**, 2629 (2009); (c) H. Jiang, J.-M. Léger, P. Guionneau, I. Huc. *Org. Lett.* **6**, 2985 (2004); (d) F. Li, Q. Gan, L. Xue, Z.-m. Wang, H. Jiang. *Tetrahedron Lett.* **50**, 2367 (2009); (e) B. Qin, X. Chen, X. Fang, Y. Shu, Y. K. Yip, Y. Yan, S. Pan, W. Q. Ong, C. Ren, H. Su, H. Zeng. *Org. Lett.* **10**, 5127 (2008); (f) L. Yang, L. Zhong, K. Yamato, X. Zhang, W. Feng, P. Deng, L. Yuan, X. C. Zeng, B. Gong. *New J. Chem.* **33**, 729 (2009); (g) C. Ren, S. Xu, J. Xu, H. Chen, H. Zeng. *Org. Lett.* **13**, 3840 (2011); (h) B. Qin, C. Sun, Y. Liu, J. Shen, R. Ye, J. Zhu, X.-F. Duan, H. Zeng. *Org. Lett.* **13**, 2270 (2011).
23. P. T. Corbett, J. Leclaire, L. Vial, K. R. West, J. L. Wietor, J. K. M. Sanders, S. Otto. *Chem. Rev.* **106**, 3652 (2006).
24. U. Lüning. *Polish J. Chem.* **82**, 1161 (2008).
25. N. Yamazaki, M. Matsumoto, F. Higashi. *J. Polym. Sci., Part A: Polym. Chem.* **13**, 1373 (1975).
26. J.-P. Sauvage, P. Gaspard (Eds.). *From Non-covalent Assemblies to Molecular Machines*, Wiley-VCH, Weinheim (2011).
27. C. P. Collier, G. Mattersteig, E. W. Wong, Y. Luo, K. Beverly, J. Sampaio, F. M. Raymo, J. F. Stoddart, J. R. Heath. *Science* **289**, 1172 (2000).
28. D. W. Steuerman, H.-R. Tseng, A. J. Peters, A. H. Flood, J. O. Jeppesen, K. A. Nielsen, J. F. Stoddart, J. R. Heath. *Angew. Chem., Int. Ed.* **43**, 6486 (2004).
29. (a) H. Li, Y.-L. Zhao, A. C. Fahrenbach, S.-Y. Kim, W. F. Paxton, J. F. Stoddart. *Org. Biomol. Chem.* **9**, 2240 (2011); (b) A. Trabolsi, A. C. Fahrenbach, S. K. Dey, A. I. Share, D. C. Friedman, S. Basu, T. B. Gasa, N. M. Khashab, S. Saha, I. Aprahamian, H. A. Khatib, A. H. Flood, J. F. Stoddart. *Chem. Commun.* **46**, 871 (2010).
30. C. J. Hawker, M. J. Fréchet. *J. Am. Chem. Soc*. **112**, 7638 (1990).

